Inorganic Chemistry

pubs.acs.org/IC

Article

A Bumper Crop of Boiling-Water-Stable Metal–Organic Frameworks from Controlled Linker Sulfuration

Wan-Ru Xian,[§] Yonghe He,[§] Yingxue Diao, Yan-Lung Wong, Hua-Qun Zhou, Sai-Li Zheng, Wei-Ming Liao, Zhengtao Xu,* and Jun He*

Cite This: https://dx.doi.org/10.1021/acs.inorgchem.0c00576

Read Online

ACCESS | Metrics & More | Article Recommendations | Supporting Information

ABSTRACT: The series of highly stable porous solids here feature systematic, regiospecific sulfur substitutions on the organic linkers for versatile functions. One major surprise lies in the controllable sequential reactions between sodium thiomethoxide (NaSMe) and octafluorobiphenyl-4,4′-dicarboxylic acid (H_2bpdc-8F; this was readily made without precious metal catalysts). Namely, 3, 4, 6, and 8 methylthio-substitutions can be respectively achieved with regiospecificity (i.e., to produce the four molecules H_2bpdc-3S5F, H_2bpdc-4S4F, H_2bpdc-6S2F, H_2bpdc-8MS). A second surprise lies in their persistent formation of the UiO-67-type net with Zr(IV) ions, e.g., even in the case of the fully sulfurated H_2bpdc-8MS. In addition to the remarkable breadth of functional control, all the Zr(IV)-based crystalline solids here are stable in boiling water (e.g., for 24 h) and in air as solventless, activated porous solids. Moreover, the thioether groups allow for convenient H_2O_2 oxidation to fine-tune the hydrophilicity and luminescence properties and improve proton conductivity.

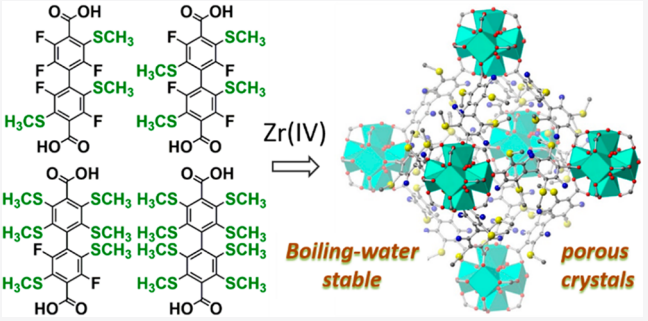

Variable pore size, variable chemical functionality, and reactivity in the crystalline medium remain major incentives in the pursuit of the diverse solids of metal–organic frameworks (MOFs).[1−12] The modular nature of MOF structures was highlighted in the earlier silver-nitrile[1,13−17] and Zn(II)-carboxylate networks[2] as well as the currently thriving Zr(IV)-based system initiated by Lillerude.[18−23] In these studies, the size and shape of the linker backbone are systematically varied to effectively impact the net topology and pore features.[24−29] On the other hand, the attachment of secondary groups (e.g., side chains) opens up intriguing horizons for novel functions and properties in the well-defined porous medium of MOF crystals.[30−35] Besides topical areas such as catalysis[36−43] and environmental remediation,[44−49] side chain groups, by sheer volume, occupy the void space so as to fine-tune the microporous features. To optimize the performances of MOF solids, it is desirable to develop versatile linker systems that can be conveniently modified in the number and function of the secondary groups.

Just such a system is described here. Building on our longstanding effort in utilizing thiolate anions as facile nucleophiles for accessing functional building blocks for framework materials,[50−54] we set eyes on the perfluoronated substrate H_2bpdc-8F (octafluorobiphenyl-4,4′-dicarboxylic acid; Figure 1): this molecule was earlier made by Miljanic et al.,[55] but Larionov et al. subsequently reported an easier synthesis[56] entailing no expensive transition metal catalysts. As an initial test, we subjected the dimethyl ester of H_2bpdc-8F to

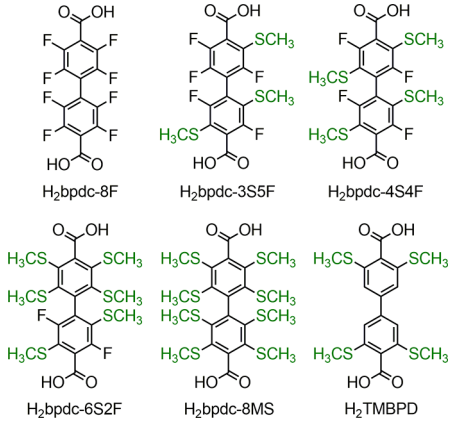

Figure 1. Molecule H_2bpdc-8F and its methylthio derivatives H_2bpdc-3S5F, H_2bpdc-4S4F, H_2bpdc-6S2F, H_2bpdc-8MS, and the known H_2TMBPD.

Received: February 22, 2020

the simple sulfur nucleophile methylthiolate (Figure S1). Surprisingly, the displacement of the fluoro groups by the sulfur groups follows a controllable sequence that allows easy isolation of each of the four isomers as shown in Figure 1 (i.e., the tri-, tetra-, hexa-, and octa-substituted products of H_2bpdc-3S5F, H_2bpdc-4S4F, H_2bpdc-6S2F, and H_2bpdc-8MS). Because of the increasing importance of the versatile sulfur groups for functionalizing the MOF host,[30] we are motivated to communicate this synthetic discovery together with the series of MOF products that also stand out for their remarkable stability in water and air.

H_2bpdc-8F was synthesized using the inexpensive reagents of $SnCl_2$, zinc powder, and $CuCl_2$ in gram scale with no need for chromatographic separation, while the degree of sulfuration can be controlled by the reactants H_2bpdc-8F/MeSNa ratio and reaction time to systematically target each of the four products (H_2bpdc-3S5F, H_2bpdc-4S4F, H_2bpdc-6S2F, and H_2bpdc-8MS) as linkers for MOF assembly. The characterization of the linker products includes solution ^{1}H, ^{19}F and ^{13}C NMR as well as single-crystal X-ray diffraction (SCXRD) studies. For example, the SCXRD structures of the MOF crystals of Pb-bpdc-4S4F and Pb-bpdc-8MS (obtained by solvothermally reacting in CH_3CN/H_2O mixed solvents $Pb(NO_3)_2$ with H_2bpdc-4S4F and H_2bpdc-8MS, respectively) unambiguously reveals the eight MeS substituents of bpdc-8MS land the *para*-substitutions of bpdc-4S4F (Figures S37 and S38). Notice that Pb-bpdc-4S4F adopts the chiral space group $P2_12_12_1$ due to the axial chirality of the biaryl linker bpdc-4S4F. The main focus is, however, presently on the Zr(IV)-based MOF products because of the distinct modularity (i.e., consistently adopting the UiO-67-type network; Figure 2) and the remarkable framework stability achieved.

Crystalline solids of Zr-bpdc-3S5F, Zr-bpdc-4S4F, and Zr-bpdc-6S2F were obtained by solvothermally reacting (in DMF solvent) $ZrCl_4$ with H_2bpdc-3S5F, H_2bpdc-4S4F, and H_2bpdc-6S2F, respectively. The phase-pure, UiO-67-type MOF products were revealed in the powder X-ray diffraction (PXRD) patterns (Figure 3). Among these, single crystals

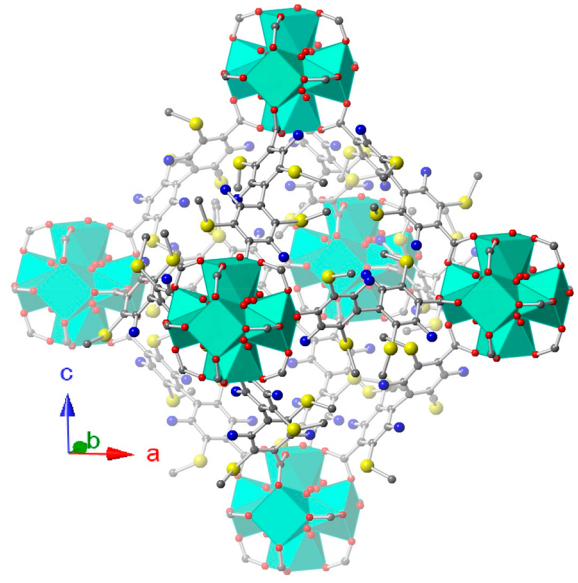

Figure 2. An octahedral cage from the single crystal structure of the Zr-bpdc-4S4F framework. The disorder of the linker molecule is not shown. Zr coordination polyhedra are displayed in cyan. Atom colors: red, O; yellow, S; gray, C; blue, F.

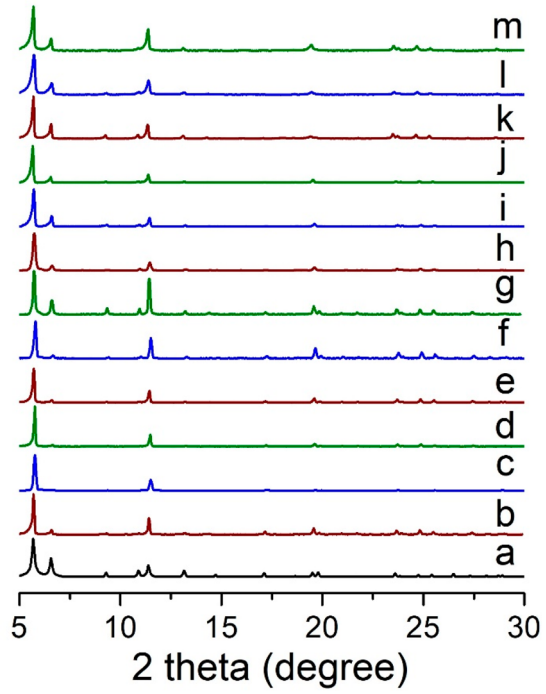

Figure 3. Powder X-ray diffraction patterns (Cu Kα, λ = 1.5418 Å) of (a) a simulation from the single crystal structure of Zr-bpdc-4S4F (single crystal data collected at 100 K); (b, e, h, k) the as-made samples of Zr-bpdc-3S5F, Zr-bpdc-4S4F, Zr-bpdc-6S2F, and Zr-bpdc-8MS, respectively; (c, f, i, l) the activated samples (Soxhlet extraction with methanol for 3 days) of Zr-bpdc-3S5F, Zr-bpdc-4S4F, Zr-bpdc-6S2F, and Zr-bpdc-8MS, respectively; (d, g, j, m) the boiling-water-treated sample of Zr-bpdc-3S5F, Zr-bpdc-4S4F, Zr-bpdc-6S2F, and Zr-bpdc-8MS, respectively.

suitable for X-ray studies were obtained for Zr-bpdc-4S4F, which unveils its isoreticular relation to the UiO-67 prototype (i.e., Zr-BPD with fcc-arrayed Zr_6O_8 units[18]) but with well-defined sulfur and fluoro functions (Figure 2). Elemental results on the activated samples (e.g., from Soxhlet extraction in methanol) can be fitted with the formulas of $Zr_6O_4(OH)_4$(bpdc-3S5F)$_{5.1}$(HCOO)$_{1.8}$(H_2O)$_2$ for Zr-bpdc-3S5F, $Zr_6O_4(OH)_4$(bpdc-4S4F)$_4$(HCOO)$_4$(H_2O)$_3$ for Zr-bpdc-4S4F, $Zr_6O_4(OH)_4$(bpdc-6S2F)$_{3.4}$(HCOO)$_{5.2}$ for Zr-bpdc-6S2F, and $Zr_6O_4(OH)_4$(bpdc-8MS)$_{3.2}$(HCOO)$_{5.6}$(CH_3OH)$_{9.5}$ for Zr-bpdc-8MS. The greater ligand deficiency observed in Zr-bpdc-8MS can be attributed to the bulkiness of the fully sulfurated bpdc-8MS linker (i.e., it is sterically more demanding to fit this linker around the Zr−O cluster).

The stability of the MOF materials is also demonstrated by both PXRD and gas sorption studies. The activated samples of Zr-bpdc-3S5F, Zr-bpdc-4S4F, Zr-bpdc-6S2F, and Zr-bpdc-8MS all exhibit long-term stability, e.g., without significant broadening of the PXRD peaks, when exposed to air in the absence of solvents (Figure 3, patterns c, f, i, l). The N_2 sorption isotherms (77 K) feature dominant type-I characteristics of microporous solids (Figure 4, panels a, c, e, g). The BET surface areas are calculated to be 986 $m^2 \cdot g^{-1}$ for Zr-bpdc-3S5F, 835 $m^2 \cdot g^{-1}$ for Zr-bpdc-4S4F, 657 $m^2 \cdot g^{-1}$ for Zr-bpdc-6S2F, and 449 $m^2 \cdot g^{-1}$ for Zr-bpdc-8MS (see also Table S1).

https://dx.doi.org/10.1021/acs.inorgchem.0c00576
Inorg. Chem. XXXX, XXX, XXX−XXX

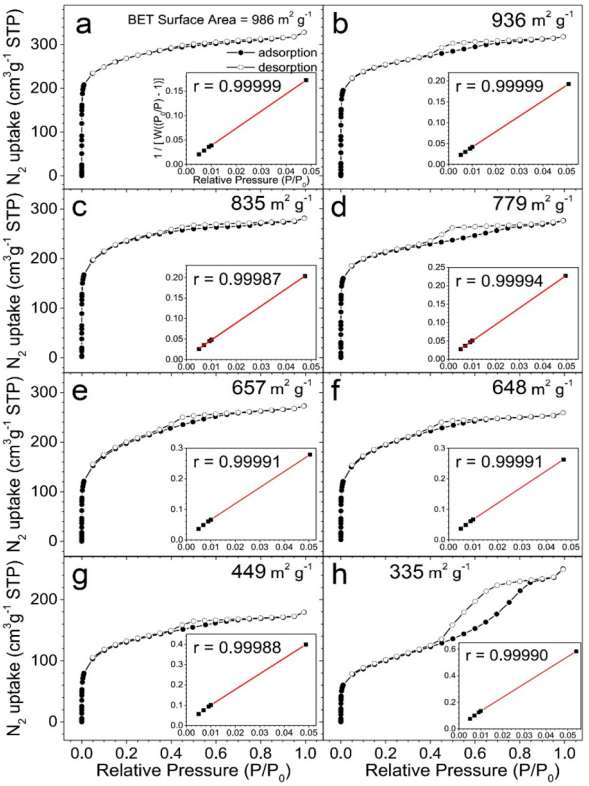

Figure 4. N_2 sorption isotherms at 77 K and BET plot (insets) for the activated MOFs: (a) Zr-bpdc-3S5F, (c) Zr-bpdc-4S4F, (e) Zr-bpdc-6S2F, and (g) Zr-bpdc-8MS and the boiling-water-treated samples of (b) Zr-bpdc-3S5F, (d) Zr-bpdc-4S4F, (f) Zr-bpdc-6S2F, and (h) Zr-bpdc-8MS.

The steadily decreasing surface areas in this series are consistent with the increasing degree of sulfuration and the resultant bulkiness of the linkers taking up more of the pore space. This trend also fits with the measured surface area and pore volume (S_{BET} = 1877 m^2/g and V_{micro} = 0.85 $cm^3\ g^{-1}$) for the unsubstituted UiO-67 prototype.[57]

The MOF samples were also found to be remarkably stable to aqueous environments. For example, even after being boiled in water (100 °C) for 24 h, the PXRD peaks of all four samples remain sharp and strong, being consistent with the native crystalline phases (Figure 3, patterns d, g, j, m). Moreover, gas sorption studies indicate that the boiling-water-treated samples continue to feature type-I isotherms characteristic of microporous solids (Figure 4, panels b, d, f, h), with the surface areas largely maintained compared with before boiling water treatment (e.g., <10% variation in surface areas): 936 $m^2{\cdot}g^{-1}$ for Zr-bpdc-3S5F, 779 $m^2{\cdot}g^{-1}$ for Zr-bpdc-4S4F, 648 $m^2{\cdot}g^{-1}$ for Zr-bpdc-6S2F, and 335 $m^2{\cdot}g^{-1}$ for Zr-bpdc-8MS. Compared with more fragile unsubstituted UiO-67 solid (e.g., crystallinity degrading upon solvent removal),[58−60] the air and water stability of this series of Zr-MOF solids, together with the recent example of ZrTMBPD, with TMBPD being 3,3′,5,5′-tetrakis(methylthio)biphenyl dicarboxylate (Figure 1),[54] demonstrate the usefulness of sulfur functions (e.g., by means of their steric shield around the metal cluster) for accessing stable MOF materials.

Postsynthetic oxidation of the Zr-bpdc-4S4F crystals is also informative. With the vigorous oxidizer of 30% H_2O_2, all four thioether groups of the linker were converted into the sulfone functions (as verified by the IR, ^1H and ^{19}F NMR spectra; Figures S40−S42), without compromising the framework lattice (e.g., PXRD in Figure S43). By comparison, thorough conversion into sulfone was not feasible in ZrTMBPD: i.e., treatment by 5% H_2O_2 led to a sulfone/sulfoxide mixture, while more stringent oxidation (e.g., by 30% H_2O_2) degraded the framework. The steric factor is obvious: in ZrTMBPD, all the S groups are crowded around the Zr_6 cluster, leaving less room for the incoming O atoms; while such crowding is lessened in Zr-bpdc-4S4F by the smaller F atoms ortho to the carboxyl donors.

The sulfone-equipped crystal (denoted as Zr-bpdc-$4SO_2$Me4F) features greatly increased hydrophilicity with a water contact angle of 64°, relative to 91° for Zr-bpdc-4S4F (Figure S44). The enhanced hydrophilicity is also consistent with the higher proton conductivities of Zr-bpdc-$4SO_2$Me4F (Figure S45), e.g., about 1.75×10^{-4} $S{\cdot}cm^{-1}$ at 80 °C and 90% relative humidity (pellet sample), representing a thousand-fold increase from the sulfide precursor Zr-bpdc-4S4F (Figures S46 and S47). The fluorescence of the H_2O_2 oxidation process is monitored to reveal an interesting dynamic (Figure 5). The Zr-bpdc-4S4F solid features blue fluorescence in moderate intensity with λ_{max} = 430 nm (λ_{ex} = 360 nm); the intensity initially goes down (λ_{max} little changed), reaching a minimum

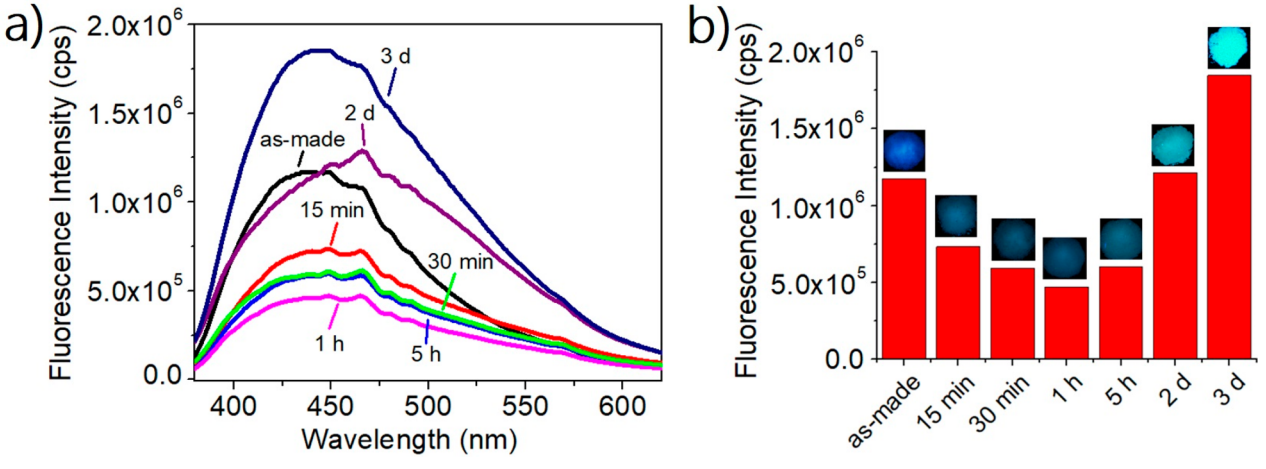

Figure 5. (a) Room temperature emission spectra (λ_{ex} = 360 nm) and (b) the bar graph of intensity against reaction time for Zr-bpdc-4S4F reacted with 30% H_2O_2 (insets: photographs of the solid samples under 360 nm radiation).

https://dx.doi.org/10.1021/acs.inorgchem.0c00576
Inorg. Chem. XXXX, XXX, XXX−XXX

(about 1/3 of the original) at 1.0 h of reaction time, after which the trend reverses to plateau (after 3 days) at twice the intensity of Zr-bpdc-4S4F, with λ_{max} also red-shifted (to about 450 nm) to feature the distinct green emission of Zr-bpdc-4SO_2Me4F. The original emission possibly arises from the coupling of the sulfide S donors and the electron-accepting biphenyl/carboxyl moieties; the initial oxidation of S (e.g., into sulfoxide) diminishes its donor character, thus weakening the luminescence. Further oxidation, however, generates multiple electropositive sulfone groups (e.g., to couple with the fluoro lone-pair electrons), which expand the conjugate system to red-shift the emission and rigidify the linker backbone for stronger luminescence.

Taken together, the significant synthetic progresses here broadly span three areas: (1) targeted linker molecule synthesis with precise control on the thioether numbers and positions installed; (2) modular, persistent formation of the prototype (UiO-67) porous frameworks stable to boiling water and air; (3) diverse postsynthetic modifications as illustrated by the tunable oxidation of the sulfide groups (all the way into the sulfone groups). Further exploration of the facile substitution of the −F groups (e.g., by conjugated or chiral nucleophiles) is warranted by the functional versatility of this platform of porous solid synthesis based on polyfluoronated aromatic substrates.

■ ASSOCIATED CONTENT

Supporting Information

The Supporting Information is available free of charge at https://pubs.acs.org/doi/10.1021/acs.inorgchem.0c00576.

General synthetic experimental details, NMR spectra, and IR, PXRD, TGA, CHN, and BET results (PDF)

Accession Codes

CCDC 1985579−1985581 contain the supplementary crystallographic data for this paper. These data can be obtained free of charge via www.ccdc.cam.ac.uk/data_request/cif, or by emailing data_request@ccdc.cam.ac.uk, or by contacting The Cambridge Crystallographic Data Centre, 12 Union Road, Cambridge CB2 1EZ, UK; fax: +44 1223 336033.

■ AUTHOR INFORMATION

Corresponding Authors

Jun He − *School of Chemical Engineering and Light Industry, Guangdong University of Technology, Guangzhou 510006, Guangdong, China;* orcid.org/0000-0001-7062-4001; Email: junhe@gdut.edu.cn

Zhengtao Xu − *Department of Chemistry, City University of Hong Kong, Kowloon, Hong Kong, China;* orcid.org/0000-0002-7408-4951; Email: zhengtao@cityu.edu.hk

Authors

Wan-Ru Xian − *School of Chemical Engineering and Light Industry, Guangdong University of Technology, Guangzhou 510006, Guangdong, China*

Yonghe He − *School of Chemical Engineering and Light Industry, Guangdong University of Technology, Guangzhou 510006, Guangdong, China*

Yingxue Diao − *Department of Chemistry, City University of Hong Kong, Kowloon, Hong Kong, China*

Yan-Lung Wong − *Department of Chemistry, City University of Hong Kong, Kowloon, Hong Kong, China*

Hua-Qun Zhou − *School of Chemical Engineering and Light Industry, Guangdong University of Technology, Guangzhou 510006, Guangdong, China*

Sai-Li Zheng − *School of Chemical Engineering and Light Industry, Guangdong University of Technology, Guangzhou 510006, Guangdong, China*

Wei-Ming Liao − *School of Chemical Engineering and Light Industry, Guangdong University of Technology, Guangzhou 510006, Guangdong, China*

Complete contact information is available at: https://pubs.acs.org/10.1021/acs.inorgchem.0c00576

Author Contributions

§W.R.X. and Y.H. contributed equally to this work.

Notes

The authors declare no competing financial interest.

■ ACKNOWLEDGMENTS

This work was funded by the Local Innovative and Research Teams Project of Guangdong Pearl River Talents Program (2017BT01Z032), National Natural Science Foundation of China (21871061, 21901046), and Science and Technology Planning Project of Guangdong Province (2017A050506051), Science and Technology Program of Guangzhou (201807010026). Z.X. acknowledges an ARG (CityU 9667168) grant.

■ REFERENCES

(1) Kiang, Y.-H.; Gardner, G. B.; Lee, S.; Xu, Z.; Lobkovsky, E. B. Variable Pore Size, Variable Chemical Functionality, and an Example of Reactivity within Porous Phenylacetylene Silver Salts. *J. Am. Chem. Soc.* **1999**, *121*, 8204−8215.

(2) Eddaoudi, M.; Kim, J.; Rosi, N.; Vodak, D.; Wachter, J.; O'Keeffe, M.; Yaghi, O. M. Systematic design of pore size and functionality in isoreticular MOFs and their application in methane storage. *Science* **2002**, *295*, 469−472.

(3) Cohen, S. M. The Postsynthetic Renaissance in Porous Solids. *J. Am. Chem. Soc.* **2017**, *139*, 2855−2863.

(4) Ali Akbar Razavi, S.; Morsali, A. Linker functionalized metal-organic frameworks. *Coord. Chem. Rev.* **2019**, *399*, 213023.

(5) Hoskins, B. F.; Robson, R. Infinite polymeric frameworks consisting of three dimensionally linked rod-like segments. *J. Am. Chem. Soc.* **1989**, *111*, 5962−5964.

(6) Kondo, M.; Yoshitomi, T.; Seki, K.; Matsuzaka, H.; Kitagawa, S. Three-dimensional framework with channeling cavities for small molecules: {[M2(4,4′-bpy)3(NO3)4].xH2O}n (M = Co, Ni, Zn). *Angew. Chem., Int. Ed. Engl.* **1997**, *36*, 1725−1727.

(7) MacGillivray, L. R.; Subramanian, S.; Zaworotko, M. J. Interwoven two- and three-dimensional coordination polymers through self-assembly of CuI cations with linear bidentate ligands. *J. Chem. Soc., Chem. Commun.* **1994**, 1325−1326.

(8) Gardner, G. B.; Venkataraman, D.; Moore, J. S.; Lee, S. Spontaneous assembly of a hinged coordination network. *Nature* **1995**, *374*, 792−795.

(9) Chui, S. S. Y.; Lo, S. M. F.; Charmant, J. P. H.; Orpen, A. G.; Williams, I. D. A chemically functionalizable nanoporous material [Cu3(TMA)2(H2O)3]n. *Science* **1999**, *283*, 1148−1150.

(10) Yaghi, O. M.; Li, G. M.; Li, H. L. Selective Binding and Removal of Guests in a Microporous Metal-Organic Framework. *Nature* **1995**, *378*, 703−706.

(11) Huang, X.; Zhang, J.; Chen, X. [Zn(bim)2]·(H2O)1.67: a metal-organic open-framework with sodalite topology. *Chin. Sci. Bull.* **2003**, *48*, 1531−1534.

(12) Gai, Y.; Chen, X.; Yang, H.; Wang, Y.; Bu, X.; Feng, P. A new strategy for constructing a disulfide-functionalized ZIF-8 analogue

using structure-directing ligand-ligand covalent interaction. *Chem. Commun.* **2018**, *54*, 12109−12112.
(13) Choe, W.; Kiang, Y. H.; Xu, Z.; Lee, S. Coordination Networks of C3v and C2v Phenylacetylene Nitriles and Silver(I) Salts: Interplay of Ligand Symmetry and Molecular Dipole Moments in the Solid State. *Chem. Mater.* **1999**, *11*, 1776−1783.
(14) Xu, Z.; Lee, S.; Kiang, Y.-H.; Mallik, A. B.; Tsomaia, N.; Mueller, K. T. A cross-linked large channel organic coordination solid. *Adv. Mater.* **2001**, *13*, 637−641.
(15) Xu, Z.; Kiang, Y.-H.; Lee, S.; Lobkovsky, E. B.; Emmott, N. Hydrophilic-to-hydrophobic volume ratios as structural determinant in small-length scale amphiphilic crystalline systems: silver salts of phenylacetylene nitriles with pendant oligo(ethylene oxide) chains. *J. Am. Chem. Soc.* **2000**, *122*, 8376−8391.
(16) Kiang, Y.-H.; Gardner, G. B.; Lee, S.; Xu, Z. Porous Siloxane Linked Phenylacetylene Nitrile Silver Salts from Solid State Dimerization and Low Polymerization. *J. Am. Chem. Soc.* **2000**, *122*, 6871−6883.
(17) Kiang, Y. H.; Lee, S.; Xu, Z.; Choe, W.; Gardner, G. B. Persistent honeycomb structures in porous and other two-component solids. *Adv. Mater.* **2000**, *12*, 767−770.
(18) Cavka, J. H.; Jakobsen, S.; Olsbye, U.; Guillou, N.; Lamberti, C.; Bordiga, S.; Lillerud, K. P. A New Zirconium Inorganic Building Brick Forming Metal Organic Frameworks with Exceptional Stability. *J. Am. Chem. Soc.* **2008**, *130*, 13850−13851.
(19) Zhang, Y.; Zhang, X.; Lyu, J.; Otake, K.-i.; Wang, X.; Redfern, L. R.; Malliakas, C. D.; Li, Z.; Islamoglu, T.; Wang, B.; Farha, O. K. A Flexible Metal-Organic Framework with 4-Connected Zr6 Nodes. *J. Am. Chem. Soc.* **2018**, *140*, 11179−11183.
(20) Pang, J.; Yuan, S.; Qin, J.; Liu, C.; Lollar, C.; Wu, M.; Yuan, D.; Zhou, H. C.; Hong, M. Control the Structure of Zr-Tetracarboxylate Frameworks through Steric Tuning. *J. Am. Chem. Soc.* **2017**, *139*, 16939−16945.
(21) Yang, P.; Shu, Y.; Zhuang, Q.; Li, Y.; Gu, J. A robust MOF-based trap with high-density active alkyl thiol for the super-efficient capture of mercury. *Chem. Commun.* **2019**, *55*, 12972−12975.
(22) Rimoldi, M.; Howarth, A. J.; DeStefano, M. R.; Lin, L.; Goswami, S.; Li, P.; Hupp, J. T.; Farha, O. K. Catalytic Zirconium/Hafnium-Based Metal-Organic Frameworks. *ACS Catal.* **2017**, *7*, 997−1014.
(23) Yuan, S.; Qin, J.-S.; Lollar, C. T.; Zhou, H.-C. Stable Metal-Organic Frameworks with Group 4 Metals: Current Status and Trends. *ACS Cent. Sci.* **2018**, *4*, 440−450.
(24) Zhang, X.; Zhang, X.; Johnson, J. A.; Chen, Y.-S.; Zhang, J. Highly Porous Zirconium Metal-Organic Frameworks with β-UH3-like Topology Based on Elongated Tetrahedral Linkers. *J. Am. Chem. Soc.* **2016**, *138*, 8380−8383.
(25) Ye, Y.; Zhao, L.; Hu, S.; Liang, A.; Li, Y.; Zhuang, Q.; Tao, G.; Gu, J. Specific detection of hypochlorite based on the size-selective effect of luminophore integrated MOF-801 synthesized by a one-pot strategy. *Dalton Trans.* **2019**, *48*, 2617−2625.
(26) Qiu, Y.-C.; Yuan, S.; Li, X.-X.; Du, D.-Y.; Wang, C.; Qin, J.-S.; Drake, H. F.; Lan, Y.-Q.; Jiang, L.; Zhou, H.-C. Face-Sharing Archimedean Solids Stacking for the Construction of Mixed-Ligand Metal-Organic Frameworks. *J. Am. Chem. Soc.* **2019**, *141*, 13841−13848.
(27) Zhai, Q.-G.; Bu, X.; Zhao, X.; Li, D.-S.; Feng, P. Pore Space Partition in Metal-Organic Frameworks. *Acc. Chem. Res.* **2017**, *50*, 407−417.
(28) Jacobsen, J.; Reinsch, H.; Stock, N. Systematic Investigations of the Transition between Framework Topologies in Ce/Zr-MOFs. *Inorg. Chem.* **2018**, *57*, 12820−12826.
(29) Waitschat, S.; Reinsch, H.; Arpacioglu, M.; Stock, N. Direct water-based synthesis and characterization of new Zr/Hf-MOFs with dodecanuclear clusters as IBUs. *CrystEngComm* **2018**, *20*, 5108−5111.
(30) He, J.; Cheng, S.; Xu, Z. Sulfur Chemistry for Stable and Electroactive Metal-Organic Frameworks: The Crosslinking Story. *Chem. - Eur. J.* **2019**, *25*, 1−10.
(31) Li, B.; Chrzanowski, M.; Zhang, Y.; Ma, S. Applications of metal-organic frameworks featuring multi-functional sites. *Coord. Chem. Rev.* **2016**, *307*, 106−129.
(32) He, J.; Zeller, M.; Hunter, A. D.; Xu, Z. Functional shakeup of metal-organic frameworks: the rise of the sidekick. *CrystEngComm* **2015**, *17*, 9254−9263.
(33) Lee, J.; Lim, D.-W.; Dekura, S.; Kitagawa, H.; Choe, W. MOP × MOF: Collaborative Combination of Metal-Organic Polyhedra and Metal-Organic Framework for Proton Conductivity. *ACS Appl. Mater. Interfaces* **2019**, *11*, 12639−12646.
(34) Nam, D.; Huh, J.; Lee, J.; Kwak, J. H.; Jeong, H. Y.; Choi, K.; Choe, W. Cross-linking Zr-based metal-organic polyhedra via postsynthetic polymerization. *Chem. Sci.* **2017**, *8*, 7765−7771.
(35) Chen, T.-F.; Han, S.-Y.; Wang, Z.-P.; Gao, H.; Wang, L.-Y.; Deng, Y.-H.; Wan, C.-Q.; Tian, Y.; Wang, Q.; Wang, G.; Li, G.-S. Modified UiO-66 frameworks with methylthio, thiol and sulfonic acid function groups: The structure and visible-light-driven photocatalytic property study. *Appl. Catal., B* **2019**, *259*, 118047.
(36) Wu, X.; Han, X.; Xu, Q.; Liu, Y.; Yuan, C.; Yang, S.; Liu, Y.; Jiang, J.; Cui, Y. Chiral BINOL-Based Covalent Organic Frameworks for Enantioselective Sensing. *J. Am. Chem. Soc.* **2019**, *141*, 7081−7089.
(37) Xia, Q.; Li, Z.; Tan, C.; Liu, Y.; Gong, W.; Cui, Y. Multivariate Metal-Organic Frameworks as Multifunctional Heterogeneous Asymmetric Catalysts for Sequential Reactions. *J. Am. Chem. Soc.* **2017**, *139*, 8259−8266.
(38) Feng, X.; Song, Y.; Li, Z.; Kaufmann, M.; Pi, Y.; Chen, J.; Xu, Z.; Zhong, L.; Wang, C.; Lin, W. Metal-Organic Framework Stabilizes A Low-Coordinate Iridium Complex for Catalytic Methane Borylation. *J. Am. Chem. Soc.* **2019**, *141*, 11196−11203.
(39) Gui, B.; Yee, K.-K.; Wong, Y.-L.; Yiu, S.-M.; Zeller, M.; Wang, C.; Xu, Z. Tackling poison and leach: catalysis by dangling thiol-palladium functions within a porous metal-organic solid. *Chem. Commun.* **2015**, *51*, 6917−6920.
(40) Yee, K.-K.; Wong, Y.-L.; Zha, M.; Adhikari, R. Y.; Tuominen, M. T.; He, J.; Xu, Z. Room-temperature acetylene hydration by a Hg(II)-laced metal-organic framework. *Chem. Commun.* **2015**, *51*, 10941−10944.
(41) Mon, M.; Rivero-Crespo, M. A.; Ferrando-Soria, J.; Vidal-Moya, A.; Boronat, M.; Leyva-Perez, A.; Corma, A.; Hernandez-Garrido, J. C.; Lopez-Haro, M.; Calvino, J. J.; Ragazzon, G.; Credi, A.; Armentano, D.; Pardo, E. Synthesis of Densely Packaged, Ultrasmall Pt02 Clusters within a Thioether-Functionalized MOF: Catalytic Activity in Industrial Reactions at Low Temperature. *Angew. Chem., Int. Ed.* **2018**, *57*, 6186−6191.
(42) Fortea-Perez, F. R.; Mon, M.; Ferrando-Soria, J.; Boronat, M.; Leyva-Perez, A.; Corma, A.; Herrera, J. M.; Osadchii, D.; Gascon, J.; Armentano, D.; Pardo, E. The MOF-driven synthesis of supported palladium clusters with catalytic activity for carbene-mediated chemistry. *Nat. Mater.* **2017**, *16*, 760−766.
(43) Qin, J.-S.; Yuan, S.; Lollar, C.; Pang, J.; Alsalme, A.; Zhou, H.-C. Stable metal-organic frameworks as a host platform for catalysis and biomimetics. *Chem. Commun.* **2018**, *54*, 4231−4249.
(44) Carboni, M.; Abney, C. W.; Liu, S.; Lin, W. Highly porous and stable metal-organic frameworks for uranium extraction. *Chem. Sci.* **2013**, *4*, 2396−2402.
(45) Yee, K.-K.; Reimer, N.; Liu, J.; Cheng, S.-Y.; Yiu, S.-M.; Weber, J.; Stock, N.; Xu, Z. Effective Mercury Sorption by Thiol-Laced Metal-Organic Frameworks: in Strong Acid and the Vapor Phase. *J. Am. Chem. Soc.* **2013**, *135*, 7795−7798.
(46) Li, M.-Q.; Wong, Y.-L.; Lum, T.-S.; Sze-Yin Leung, K.; Lam, P. K. S.; Xu, Z. Dense thiol arrays for metal-organic frameworks: boiling water stability, Hg removal beyond 2 ppb and facile crosslinking. *J. Mater. Chem. A* **2018**, *6*, 14566−14570.
(47) Zha, M.; Liu, J.; Wong, Y.-L.; Xu, Z. Extraction of palladium from nuclear waste-like acidic solutions by a metal-organic framework with sulfur and alkene functions. *J. Mater. Chem. A* **2015**, *3*, 3928−3934.

https://dx.doi.org/10.1021/acs.inorgchem.0c00576
Inorg. Chem. XXXX, XXX, XXX−XXX

(48) Hou, Y.-L.; Yee, K.-K.; Wong, Y.-L.; Zha, M.; He, J.; Zeller, M.; Hunter, A. D.; Yang, K.; Xu, Z. Metalation Triggers Single Crystalline Order in a Porous Solid. *J. Am. Chem. Soc.* **2016**, *138*, 14852−14855.
(49) Mon, M.; Lloret, F.; Ferrando-Soria, J.; Martí-Gastaldo, C.; Armentano, D.; Pardo, E. Selective and Efficient Removal of Mercury from Aqueous Media with the Highly Flexible Arms of a BioMOF. *Angew. Chem., Int. Ed.* **2016**, *55*, 11167−11172.
(50) Li, K.; Xu, Z.; Xu, H.; Ryan, J. M. Semiconductive Coordination Networks from 2,3,6,7,10,11-Hexakis(alkylthio)-triphenylenes and Bismuth(III) Halides: Synthesis, Structure-Property Relations, and Solution Processing. *Chem. Mater.* **2005**, *17*, 4426−4437.
(51) Li, K.; Xu, Z.; Xu, H.; Carroll, P. J.; Fettinger, J. C. Three-Dimensional Nets from Star-Shaped Hexakis(arylthio)triphenylene Molecules and Silver(I) Salts. *Inorg. Chem.* **2006**, *45*, 1032−1037.
(52) Cui, J.; Xu, Z. An electroactive porous network from covalent metal-dithiolene links. *Chem. Commun.* **2014**, *50*, 3986−3988.
(53) Zhou, X.-P.; Xu, Z.; Zeller, M.; Hunter, A. D.; Chui, S. S.-Y.; Che, C.-M. Coordination Networks from a Bifunctional Molecule Containing Carboxyl and Thioether Groups. *Inorg. Chem.* **2008**, *47*, 7459−7461.
(54) Wong, Y.-L.; Yee, K.-K.; Hou, Y.-L.; Li, J.; Wang, Z.; Zeller, M.; Hunter, A. D.; Xu, Z. Single-Crystalline UiO-67-Type Porous Network Stable to Boiling Water, Solvent Loss, and Oxidation. *Inorg. Chem.* **2018**, *57*, 6198−6201.
(55) Chen, T.-H.; Popov, I.; Zenasni, O.; Daugulis, O.; Miljanic, O. S. Superhydrophobic perfluorinated metal-organic frameworks. *Chem. Commun.* **2013**, *49*, 6846−6848.
(56) Larionov, S. V.; Myachina, L. I.; Sheludyakova, L. A.; Korolkov, I. V.; Rakhmanova, M. I.; Plyusnin, P. E.; Vinogradov, A. S.; Karpov, V. M.; Platonov, V. E.; Fadeeva, V. P. Synthesis of Octafluor-obiphenyl-4,4′-dicarboxylic acid and photoluminescent compounds based thereon. *Russ. J. Gen. Chem.* **2015**, *85*, 1617−1622.
(57) Chavan, S.; Vitillo, J. G.; Gianolio, D.; Zavorotynska, O.; Civalleri, B.; Jakobsen, S.; Nilsen, M. H.; Valenzano, L.; Lamberti, C.; Lillerud, K. P.; Bordiga, S. H2storage in isostructural UiO-67 and UiO-66 MOFs. *Phys. Chem. Chem. Phys.* **2012**, *14*, 1614−1626.
(58) DeCoste, J. B.; Peterson, G. W.; Jasuja, H.; Glover, T. G.; Huang, Y.-g.; Walton, K. S. Stability and degradation mechanisms of metal-organic frameworks containing the Zr6O4(OH)4 secondary building unit. *J. Mater. Chem. A* **2013**, *1*, 5642−5650.
(59) Mondloch, J. E.; Katz, M. J.; Planas, N.; Semrouni, D.; Gagliardi, L.; Hupp, J. T.; Farha, O. K. Are Zr_6-based MOFs water stable? Linker hydrolysis vs. capillary-force-driven channel collapse. *Chem. Commun.* **2014**, *50*, 8944−8946.
(60) Lawrence, M. C.; Schneider, C.; Katz, M. J. Determining the structural stability of UiO-67 with respect to time: a solid-state NMR investigation. *Chem. Commun.* **2016**, *52*, 4971−4974.

https://dx.doi.org/10.1021/acs.inorgchem.0c00576
Inorg. Chem. XXXX, XXX, XXX−XXX